The leader protein of Theiler's virus prevents the activation of PKR by dsRNA

Fabian Borghese [1], Frédéric Sorgeloos [1], Teresa Cesaro[1] and Thomas Michiels [1#]

1. Université catholique de Louvain, de Duve Institute, VIRO B1.74.07,
74, avenue Hippocrate, B-1200, Brussels, Belgium.

Running title: PKR inhibition by TMEV

Keywords: Theiler's murine encephalomyelitis virus, PKR, leader protein, stress granules, picornavirus, *Cardiovirus*, double-stranded RNA.
Words in abstract: 209
Words in "importance" section: 134
Words in text: 3948

 # Address for correspondence:
Pr. Thomas Michiels
UCLouvain
de Duve Institute
VIRO – B1.74.07
74, avenue Hipprocrate, B-1200, Brussels, Belgium
Phone: +32 2 764 74 29
Fax: +32 2 764 74 95
e-mail: thomas.michiels@uclouvain.be

Abstract :

Leader (L) proteins encoded by cardioviruses are multifunctional proteins that contribute to innate immunity evasion. L proteins of Theiler's murine encephalomyelitis virus (TMEV), Saffold virus (SAFV) and Encephalomyocarditis virus (EMCV) were reported to inhibit stress granule assembly in infected cells. Here, we show that TMEV L can act at two levels in the stress granule formation pathway: on the one hand, it can inhibit sodium arsenite-induced stress granule assembly without preventing eIF2α phosphorylation, thus acting downstream of eIF2α; on the other hand, it can inhibit double-stranded RNA-activated protein kinase (PKR) activation and the consequent PKR-mediated eIF2α phosphorylation. Interestingly, co-immunostaining experiments revealed that PKR co-localizes with viral double-stranded RNA (dsRNA) in cells infected with L-mutant viruses but not in cells infected with the wild-type virus. Furthermore, PKR co-precipitated with dsRNA from cells infected with L-mutant viruses significantly more than from cells infected with the wild-type virus. These data strongly suggest that L blocks PKR activation by preventing the interaction between PKR and viral dsRNA. In infected cells, L also rendered PKR refractory to subsequent activation by poly(I:C). No interaction was however observed between L and either dsRNA or PKR. Taken together, our results suggest that, unlike other viral proteins, L indirectly acts on PKR to negatively regulate its responsiveness to dsRNA.

Importance

The leader (L) protein encoded by cardioviruses is a very short multifunctional protein that contributes to evasion of the host innate immune response. This protein notably prevents the formation of stress granules in infected cells. Using Theiler's virus as a model, we show that

L proteins can act at two levels in the stress response pathway leading to stress granule formation, the most striking one being the inhibition of double-stranded RNA-activated protein kinase (PKR) activation. Interestingly, the leader protein appears to inhibit PKR via a novel mechanism, by rendering this kinase unable to detect double-stranded RNA, its typical activator. Unlike other viral proteins such as influenza virus NS1, the leader protein appears to interact neither with PKR nor with double stranded RNA, suggesting that it acts indirectly, to trigger the inhibition of the kinase.

Introduction :

Theiler's Murine Encephalomyelitis virus (TMEV or Theiler's virus) belongs to the species *Theilovirus*, within the genus *Cardiovirus* from the family *Picornaviridae*. The DA strain of TMEV is known to produce a persistent infection of the central nervous system of the mouse. This infection leads to chronic demyelinating lesions reminiscent of those found in multiple sclerosis patients (1, 2). Other cardioviruses are Saffold virus (SAFV), a TMEV-related virus isolated from humans, and Encephalomyocarditis virus (EMCV), including the mengovirus strain.

The genome of cardioviruses consists of one non-segmented positive-stranded RNA molecule of approximately 8 kb. It encodes a polyprotein that is processed to generate the structural and non-structural proteins. A small protein (of about 70 amino acids) is cleaved off from the amino-terminal end of the polyprotein and is therefore called leader (L) protein. Cardiovirus L proteins are closely related multifunctional proteins shown to interfere with critical cellular processes (3) such as type I interferon and chemokine production (4, 5), nucleocytoplasmic trafficking (6-12), apoptosis (13, 14), and mitogen-activated protein (MAP) kinase activity

(15). Several domains have been defined in L: i) an amino-terminal zinc finger (CHCC), ii) a central glutamate/aspartate-rich domain that confers a very low isoelectric point (3.8) to the protein and that was shown in the case of EMCV to interact with Ran GTPase (16), and iii) a carboxy-terminal domain, only found in the *Theilovirus* species (TMEV and SAFV) and therefore called Theilo domain (17). Mutations introduced in either the zinc finger or the Theilo domain affect all the known activities of Theiloviruses L proteins (17). We and others previously reported that stress granules (SG) appear in cells infected with L-mutant, but not wild-type TMEV or mengovirus (18, 19). Therefore, *Cardiovirus* infection is a stimulus that triggers SG assembly, which is simultaneously blocked by the L protein. Stress granules (SG) are cytoplasmic aggregates of stalled mRNA translation complexes that form in cells exposed to different cellular stresses (20). In addition to their obvious role in the stress-induced translational blockade, SG are considered to serve as a platform for innate immunity signaling (21). Accordingly, cytoplasmic pathogen sensors such as RIG-I, MDA5 and PKR have been detected in virus-induced SGs (19, 21), and inhibition of SG assembly in response to ΔNS1-IAV and EMCV infection correlated with decreased type I interferon transcription (21, 22). It is thus not surprising that many viruses have developed strategies to inhibit SG assembly (reviewed in (23)).

The main event triggering SG assembly is the phosphorylation of the alpha subunit of the eukaryotic initiation factor 2 (eIF2α) by stress-activated kinases (24). Four mammalian eIF2α kinases have been identified : PKR, PERK, GCN2 and HRI. PKR is a well-known antiviral kinase whose expression is up-regulated by type I interferons and whose catalytic activity is activated by double-stranded RNA, a common by-product of viral replication (reviewed in (25)). Once activated, PKR phosphorylates eIF2α and this leads to inhibition of mRNA translation initiation. PKR contains two amino-terminal dsRNA binding domains (dsRBD)

and a carboxy-terminal catalytic protein kinase domain. Binding of dsRNA induces PKR homodimerization, trans-phosphorylation on various Ser and Thr residues, leading to full activation of the kinase. Phosphorylation of Thr446 and Thr451, located in the activation loop, is crucial for PKR activation (26) and can therefore be used as a marker to monitor the activation status of PKR. As PKR activation leads to translation arrest, many viruses evolved to antagonize PKR activity. Examples of viral countermeasures include the production of dsRNA binding proteins to prevent its detection by PKR (27, 28), triggering lysosome- (29) or proteasome-mediated (30, 31) PKR degradation, limiting the PKR-activating dsRNA or defective interfering particles production (32, 33), production of RNA secondary structures that bind to but do not activate PKR (34, 35), direct binding of a viral protein to PKR to prevent dimerization or inhibit catalytic activity (36), and recruitment of a cellular phosphatase to dephosphorylate the PKR substrate, eIF2α (37).

Using $PKR^{-/-}$ mouse embryonic fibroblasts, Langereis *et al*. showed that PKR was required for the formation of SG after infection with a mengovirus carrying a mutation in the zinc-finger domain of L (L^{Zn}). On the other hand, Ng *et al.* (22) reported that wild-type EMCV infection triggers transient SG formation and then inhibited the process by G3BP1 cleavage at late stages of infection, in a way similar to that used by Poliovirus. In G3BP1/2 double KO cells, L^{Zn} mengovirus infection failed to trigger SG formation whereas it still triggered PKR activation (38).

Using TMEV as a model, we further explored the mechanism by which the leader proteins of cardioviruses inhibit infection-induced SG. We show that L can act at two independent steps in the SG formation pathway. Importantly, our data suggest that L can act on PKR activation, by rendering PKR insensitive to the presence of double stranded RNA.

Material & methods

Cells and viruses.

HeLa cells used in this study (kindly provided by R.H. Silverman) were of the HeLa M subclone, which reportedly has low endogenous RNase L activity (39). They were maintained in Dulbecco's modified Eagle medium (Lonza) supplemented with 10% fetal calf serum (MP Biomedicals), 100 IU penicillin/ml, and 100 µg streptomycin/ml. BHK-21 cells (ATCC) were cultured in Glasgow's modified Eagle's medium (GMEM) (Sigma) supplemented with 10% newborn bovine serum (Gibco), 100 IU penicillin/ml, 100 µg streptomycin/ml (Lonza), and 2.6 g of tryptose phosphate broth per liter (Difco).

The virus referred to as wild-type in this study is named KJ6 and is a derivative of the TMEV DA1 persistent strain, which expresses the wild-type L protein and harbors capsid mutations that adapt the virus to infect L929 cells efficiently (40). L-mutant viruses derived from KJ6 are TM659, carrying mutations disrupting the L zinc finger (L^{Zn}) (4), and FB09, carrying a M60V substitution in the Theilo domain (L^{M60V}) (17). KJ7 (ΔL-GFP) is a KJ6-derivative carrying the GFP-coding sequence between codons 5 and 67 of the L-coding region.
TMEV variants expressing a 3xFLAG-tagged L protein were obtained by cloning a 3xFLAG-coding sequence 5' to the L protein initiation codon in the plasmids carrying the full-length cDNA of viruses KJ6 (pKJ6), TM659 (pTM659) and pFB09 (18). Resulting plasmids bearing the cDNA of 3xFLAG-L^{wt} 3xFLAG-L^{Zn} and 3xFLAG L^{M60V} viruses were called pTM994, pTM1016 and pTM1017 respectively. For mengovirus, the FLAG sequence and Zn finger mutations (C17A-C19A) were introduced in the attenuated strain derived from pMC24 (41), kindly provided by Ann Palmenberg. Viruses were produced by reverse genetics from these

plasmid constructs. Viruses were titrated by plaque assay on BHK-21 cells and, unless otherwise indicated, infections were performed at 10 PFU per cell for the indicated time. Viruses used in this study are listed in Table 1.

Immunostaining

Immunostainings were performed on cells that were cultivated on glass coverslips treated with poly-L-lysine and placed in 24-well plates. Prior to immunostaining, cells were fixed for 5-10 min in 300 µl of phosphate-buffered saline (PBS) containing 4% paraformaldehyde (PFA). Cells were then washed in 500 µl of PBS and permeabilized for 5 min at room temperature in 500 µl of PBS-0.1% Triton X-100. Blocking occurred for 1 h at room temperature in 300 µl of TNB blocking reagent (Perkin Elmer). Cells were next incubated with the primary antibody diluted in TNB at the following dilutions: TMEV VP1 (mouse; F12B3 clone; a kind gift of M. Brahic), 1/10; anti-TMEV capsid (rabbit polyclonal antibody; a kind gift of M. Brahic), 1/500; eIF3 (goat; Santa Cruz sc-16377), 1/200-1/800; J2 (mouse, anti-double-stranded RNA [anti-dsRNA], English & Scientific Consulting Bt.), 1/200; PKR (rabbit, GTX 61151, Genetex), 1/250. After 1 h incubation at room temperature, cells were washed 3 times for 5 min in 500 µl PBS–0.1% Tween 20. Secondary antibodies (Alexa Fluor 488- or 594-conjugated antibodies; Invitrogen) were incubated for 1 h at a 1/800 dilution in TNB. Finally, cells were washed 3 times in 500 µl PBS–0.1% Tween 20 and mounted with Mowiol for fluorescence microscopy analyses.

Fluorescence microscopy was performed with a DMIRB inverted microscope (Leica) equipped with a high-resolution AxioCam MRm digital camera (Zeiss), or with a spinning disk confocal microscope (Zeiss). Intensity, contrast, and color balance of images were equally equilibrated across conditions using ImageJ or Adobe Photoshop.

Western blotting

Proteins extracted in 1x Laemmli buffer were heated for 5 minutes at 95 °C, run on Tris-glycine-sodium dodecyl sulfate (8 or 10%) polyacrylamide gels and transferred onto nitrocellulose or poly(vinylidene fluoride) membranes. Blockage was performed in PBS-5% nonfat dry milk, or in PBS- 5% BSA for detection of phosphorylated peptides. The Supersignal enhancer kit (Pierce) was used with nitrocellulose membranes to improve detection of the L protein. Primary antibodies were anti-VP1 (see above), anti-phospho-eIF2α (rabbit, Cell Signaling #3597), anti-eIF2α (rabbit, Cell Signaling #9722), anti-PKR (rabbit, GTX61151, Genetex or 18244-1-AP, Proteintech), anti-phospho T446 PKR (rabbit, GTX 61049, Genetex/ Ab32036, Abcam), anti-phospho T451 (rabbit, GTX 61867, Genetex/ Ab81303, Abcam), anti-β actin (mouse, Sigma-Aldrich A5441), anti-L (rabbit, home- made polyclonal anti-peptide antibody), and anti-TMEV 3D polymerase (rabbit, kindly provided by M. Brahic). All primary antibodies were used at 1/1000 dilution in PBS-nonfat dry milk or PBS-BSA. Primary antibodies were detected using goat anti-rabbit, or goat anti-mouse IgG (H+L) HRP-conjugated antibodies (1/1000, Dako). Secondary antibodies were detected with SuperSignal Chemoluminescent Substrates (Thermo Scientific).

Pharmacological inhibition of PKR

Mock- or infected-cells were treated sequentially with increasing concentrations of C16 (Imidazolo-oxindole – I9785, Sigma). A first time at 1 hour post-infection with 1μM of C16 diluted in DMSO, and a second time at $7^{1/2}$h post-infection with 10 μM to give an inhibitory boost. Cells were fixed for immunostaining or harvested for Western blot analyses at 10 hours post-infection.

Knockdown of PKR expression

Three different shRNAs targeting PKR were selected from the Sigma mission collection (ref. TRCN0000001379 = shRNA1, TRCN0000001381 = shRNA2, TRCN000019400 = shRNA3) and cloned in the pLKO.1 lentiviral vector following Addgene instructions (see Addgene plasmid 10878. Protocol Version 1.0). HeLa cells were then transduced with the corresponding lentiviruses produced from these vectors and selection of transduced cells was performed with increasing concentrations of puromycin (2 to 4 μg/ml). Efficacy of the knockdown was tested by Western blot.

Immunoprecipitation

Cells cultured in 10 cm dishes (Sarstedt) were washed twice with cold PBS and lysed with 800 µl of lysis buffer per dish (150 mM NaCl, 50 mM Tris, 1 mM EDTA, 1% NP40, 1 mM PMSF, 1/1600 Ribolock RNase inhibitor, 1 tablet of Pierce phosphatase/protease inhibitor cocktail (#88669) per 10 ml of lysis buffer, pH 7.5). Cell lysates were harvested in 1.5 ml tubes, homogenized with 18G or 25G syringes, and cleared by centrifugation at 12 000 x g for 10 min at 4°C. Supernatants were then transferred to new 1.5 ml tubes and a sample of 80 µl per condition was mixed with 40 µl of 3x Laemmli buffer as a control for the total cell lysate. Remaining samples were cleared 3 times with 15 µl of protein A/G UltraLink Resin (50% slurry) (Pierce), and incubated overnight on a rotating wheel at 4°C with a 1/100 dilution of the adequate primary antibody (same antibodies as those described in the Western blotting and immunostaining sections). The following day, 50 µl of protein A/G UltraLink Resin (50% slurry) were added to the samples. These were kept on a rotating wheel at 4°C for 2 hours. Beads were washed 3 times with lysis buffer and resuspended in 50 µl of Laemmli buffer (1,5x) for Western blot analyses. For 3xFLAG-L immunoprecipitations, cells grown in 6 cm dishes were collected in 300 µl of lysis buffer. Lysates were cleared once for 30 min with 20 µl of protein A/G UltraLink Resin (50% slurry) (Pierce) and immunoprecipitation was

performed by incubating lysates with 25µl anti-FLAG magnetic beads (Sigma) for 2 hours at 4°C. Other steps were as above.

Poly(I:C) transfection

Cells seeded in a 24-well plate were transfected by dropwise deposition of a mix containing 45 µl of transfection reagent (Lipofectamine 2000) and 7.5 µl of poly(I:C) (stock at 2 mg/ml) diluted in 1.5 ml of DMEM (Lonza). Transfected cells were harvested $4^{1/2}$h after transfection.

Results

TMEV-induced stress granule assembly correlates with eIF2α phosphorylation and PKR activation.

We first confirmed previous observations showing that SGs are formed in cells infected with TMEV derivatives carrying mutations in either the zinc finger (L^{Zn}) or the Theilo domain (L^{M60V}) of the L protein, but not in cells infected with wild-type TMEV (L^{WT}) (Fig. 1A). We also examined the phosphorylation status of eIF2α (Ser51) and of PKR (Thr446 and 451) in infected cells. Western blots presented in Fig. 1B show that, in cells infected with L-mutant viruses, SG assembly correlates with eIF2α phosphorylation and PKR activation. Our data therefore suggest that L inhibits SG assembly by blocking PKR activation and the consequent eIF2α phosphorylation.

PKR is responsible for TMEV-induced eIF2α phosphorylation and stress granule assembly.

250 To test whether PKR was indeed the kinase responsible for SG formation in cells infected
251 with L-mutant TMEV, we used both pharmacological inhibition of PKR and knock-down of
252 PKR expression. Fig. 2A shows that the PKR inhibitory compound 16 (C16), an ATP
253 competitor, effectively decreases TMEV-induced PKR activation (i.e., phosphorylation of
254 both T446 and T451) and eIF2α phosphorylation. This inhibition of PKR activity was
255 sufficient to block SG assembly induced by both TMEV-L^{Zn} and TMEV-L^{M60V} (Fig. 2B). At
256 the concentration used, C16 did not prevent eIF2α phosphorylation and SG assembly induced
257 by sodium arsenite, which mostly acts through the kinase HRI (42).
258 To confirm that PKR was the cause of SG formation in TMEV-infected cells, we transduced
259 HeLa cells with lentiviral vectors coding for three different short hairpin RNAs (shRNAs)
260 directed against PKR mRNA. All three shRNAs triggered a strong inhibition of PKR
261 expression (Fig. 3A). We chose to continue our experiments with shRNA 2 and 3 because
262 some residual expression of PKR could be detected with shRNA 1 (not shown). As shown in
263 figure 3B and 3C, shRNA 3 strongly inhibited PKR expression, eIF2α phosphorylation and
264 SG assembly in response to TMEV-L^{Zn} or TMEV-L^{M60V} infection. Importantly, PKR
265 inhibition and infection did not prevent eIF2α phosphorylation and SG assembly in response
266 to arsenite treatment (Fig. 3C, bottom panel). Similar results were obtained with shRNA 2,
267 while some stress granules were still detectable with shRNA 1 in agreement with the residual
268 expression of PKR observed with this shRNA (not shown).
269 Altogether, these results show that the L protein of TMEV inhibits stress granule assembly by
270 blocking PKR activation.
271
272 **L acts at two levels to inhibit SG formation**
273 The above data (Figures 2 and 3) suggest that L can prevent PKR activation. We previously
274 observed, however, that in both infected and transfected cells, L^{WT} also prevented the

formation of sodium arsenite-induced SG, suggesting that L was acting downstream of PKR-mediated eIF2α phosphorylation (18). In the case of mengovirus, it was reported that, in cells infected with the L^{Zn} mengovirus mutant, eIF2α was phosphorylated in a PKR-dependent fashion and that this eIF2α phosphorylation was inhibited by L (19). It was therefore unclear whether L acted upstream or downstream of PKR activation.

As shown in Fig. 4 (A, D), and in agreement with our previous report (18), infection with L^{WT} TMEV consistently suppressed SG formation induced by sodium arsenite treatment. In this case however, L did not prevent eIF2α phosphorylation (Fig. 4B-C). These data confirm that L can act downstream of PKR to inhibit SG formation.

On the other hand, we confirmed that L was also acting on PKR activation, thus preventing PKR Thr446 phosphorylation. As shown in Fig. 4E-F, both mengovirus and TMEV L^{WT} inhibited PKR phosphorylation in infected cells, contrary to L mutants.

We conclude that the L protein can act both upstream and downstream of the PKR-mediated eIF2α phosphorylation step. Given the strong antagonism of L on PKR activation, we further examined the mechanism of this inhibition.

PKR is an antagonist of TMEV replication

We compared the replication levels of wild-type and L-mutant viruses in control and in PKR-knocked down HeLa cells. In agreement with the data reported for mengovirus (38), Figure 5 shows that the absence of PKR has a modest positive influence on replication of wild-type TMEV but a strong impact on L^{Zn} and L^{M60V} -mutant virus replication. Thus, PKR is an antagonist of TMEV replication and its inhibition by L is critical for optimal TMEV infection.

The L protein prevents the interaction between viral dsRNA and PKR.

299 We next investigated the mechanisms of PKR inhibition by L. First, we sought for a potential
300 interaction between L and PKR by co-immunoprecipitation. Immunoprecipitation of L^{WT}
301 from cells infected with a recombinant virus expressing a 3xFLAG-tagged L^{WT} protein failed
302 to reveal any interaction between TMEV-L and PKR although this virus fairly inhibited PKR
303 activation (Fig. 6A). Reineke et al. (43, 44) reported that SG-located G3BP1 could be
304 involved in the activation of PKR through formation of heterotrimeric complex also involving
305 Caprin1. However, as for PKR, co-immunoprecipitation experiments failed to reveal any
306 interaction between L and G3BP1 (Fig. 6A).
307 Next, we analyzed the localization of PKR in infected cells by immunostaining. Interestingly,
308 in cells infected with L-mutant viruses (L^{Zn} and L^{M60V}), PKR was markedly redistributed to
309 cytoplasmic granules where it partly co-localized with dsRNA. In sharp contrast, in cells
310 infected with the wild type virus, PKR displayed a diffuse staining and did not clearly co-
311 localize with dsRNA (Fig. 6B). In cells infected with the L^{M60V} mutant virus, PKR was
312 detected in partially distinct groups of granules: (i) conspicuous granules likely corresponding
313 to bona fide SG, often perinuclear, containing G3BP1, eIF3 and PKR and (ii) generally more
314 diffuse granules containing dsRNA, PKR, and some extent of G3BP1 (Fig. 6C-D). The lack
315 of PKR relocalization to dsRNA-containing granules in L^{WT}-virus infected cells suggests that
316 L blocks PKR activation by preventing its association with viral dsRNA.
317 To test the association of PKR with dsRNA in another setting, we immunoprecipitated
318 dsRNA from infected cell lysates and examined PKR co-immunoprecipitation. Fig. 6E shows
319 that PKR co-precipitates with dsRNA in samples infected with L-mutant viruses significantly
320 more than in samples infected with the wild-type virus. Thus, wild-type TMEV L protein
321 inhibits PKR interaction with viral dsRNA.

322 In the same experiment, we analyzed whether L^{WT} would bind viral dsRNA and thereby
323 prevent its detection by PKR. However, neither L^{WT} nor L^{Zn} nor L^{M60V} co-
324 immunoprecipitated with dsRNA (Fig. 6E).
325
326 **The L protein dampens the responsiveness of PKR to dsRNA**
327 As L appeared to interact neither with dsRNA nor with PKR, we were puzzled by the way L
328 may impede dsRNA recognition by PKR. One the one hand, L may act by preventing PKR
329 access to dsRNA (for example by reshaping or hiding viral replication complexes). On the
330 other hand, L may indirectly modify PKR to render this kinase insensitive to dsRNA. In the
331 first hypothesis, PKR would keep the potential to become activated by another stimulus (*e.g.*
332 poly(I:C)). In the second hypothesis (true PKR inhibition), PKR should be refractory to
333 poly(I:C) activation in cells infected with the wild-type virus. Therefore, we compared PKR
334 activation in response to poly(I:C) transfection in mock-infected cells and in cells infected
335 with L^{WT} or L^{Zn} viruses. Figure 7 (A-B) shows that PKR activation in response to poly(I:C)
336 was significantly decreased in cells infected with the wild-type virus. In contrast, PKR was
337 hyper phosphorylated in L^{Zn}-infected cells, showing that infection *per se* did not prevent PKR
338 activation by poly(I:C).
339 The inactive status of PKR in cells infected with the wild-type virus was confirmed in a co-
340 infection experiment. HeLa cells were infected with a wild-type virus (L^{WT}), with KJ7, a
341 TMEV derivative expressing GFP instead of L (ΔL-GFP), or co-infected with both viruses.
342 As expected, the ΔL-GFP mutant virus triggered PKR redistribution and phosphorylation (Fig.
343 7C-D). After co-infection with the L^{WT} virus, PKR phosphorylation was inhibited (Fig. 7C)
344 and PKR did not relocalize to cytoplasmic punctae in ΔL-GFP-infected cells (Fig. 7D).
345 Therefore, we concluded that the L protein of TMEV exerts a specific action that dampens the
346 responsiveness of PKR to dsRNA.

Discussion

We showed that TMEV L can inhibit SG formation by acting on the stress response both downstream of eIF2α phosphorylation and at the level of PKR activation. We then focused our analysis on the mechanism of PKR inhibition. PKR is a well-known interferon-stimulated gene product that restricts viral translation/replication through eIF2α phosphorylation and consequent inhibition of the cellular translation machinery. Accordingly, as previously observed in the case of mengovirus (19), PKR exerts a strong inhibitory effect on TMEV replication, which is counteracted by L.

Several data concur to suggest that L acts by preventing PKR association with dsRNA: i) PKR co-immunoprecipitated with dsRNA from cells infected with L^{Zn} or L^{M60V} significantly more than from cells infected with L^{WT} viruses (Fig. 6E); ii) PKR relocalized to punctate cytoplasmic dsRNA clusters after L-mutant but not L^{WT} virus infection (Fig. 6B); iii) L^{WT} decreased PKR activation by poly(I:C) (Fig. 7A-B); iv) L^{WT} suppressed PKR activation in cells that were co-infected with L^{WT} and L-mutant viruses (Fig. 7C).

Other viral proteins such as NS1 (influenza), or E3L (vaccinia), were shown to block dsRNA-mediated PKR activation (28, 45). These proteins possess a dsRNA binding domain (DRBD) that competes with PKR for dsRNA binding. In the case of cardioviruses, the leader sequence does not contain any putative dsRNA binding domain and dsRNA immunoprecipitation from TMEV-infected cells failed to reveal any interaction between L and dsRNA. Moreover, sequestration of dsRNA by L is unlikely because TMEV mutants that express truncated L* proteins (L* is an RNase L antagonist) but still express L^{WT} do not

371 inhibit the RNase L pathway (46), which depends on dsRNA detection by oligoadenylate
372 synthetases.
373 Alternatively, PKR inhibition may result from L binding to PKR DRBDs, thereby obstructing
374 dsRNA recognition. However, experimental evidence does not support this mechanism since
375 we did not detect any interaction between the L protein and PKR.
376 Thus, the L-induced PKR inability to interact with dsRNA may result from an indirect
377 mechanism. Post-translational modifications of PKR that impact its activity have been
378 described; ISGylation of lysine residues in the DRBD was shown to activate PKR
379 independently of dsRNA (47), and SUMOylation of other lysine residues was shown to be
380 important for efficient dsRNA binding and activation (48, 49). However, such post-
381 translational modification by covalent linkage of small proteins is unlikely to explain L
382 activity because the migration of PKR was not shifted in Western blots in samples from L^{WT}-
383 infected cells.
384 Many phosphorylatable residues (Ser, Thr and Tyr) are present in the DRBD of PKR. It is
385 unclear if, and how, these residues regulate the activity of PKR. However, an appealing
386 possibility is that phosphorylation of some of these residues dampens the capacity of PKR to
387 bind dsRNA, and that L triggers their phosphorylation by acting on cellular kinases or
388 phosphatases. The involvement of a cellular kinase in the activities of L is supported by the
389 work of Porter *et al*. (15) who showed the involvement of MAP kinases in L-mediated
390 activities.
391 The C protein of Measles virus (MV) was shown to prevent PKR activation without targeting
392 the classical PKR activation pathway (50). The mechanism exploits the cellular adenosine
393 deaminase ADAR1, a dsRNA editing enzyme that structurally destabilizes endogenous
394 dsRNA (e.g, transcripts containing inverted repeats in their 3'UTR) in order to avoid aberrant
395 activation of cellular dsRNA sensors such as Mda5, RIG-I and PKR (51). In an elegant paper,

Pfaller *et al.* demonstrated that MV C protein regulates the amount of viral dsRNA and of defective interfering (DI) genomes that are produced during MV replication (52). They proposed that C protein acts on viral polymerase processivity and thereby contributes to maintain aberrant viral dsRNA levels low enough to allow their destabilization by ADAR1 and prevent PKR activation (32). The C protein of Sendai virus, another paramyxovirus, was found to act in a similar fashion, by limiting dsRNA generation in the course of viral replication (33). Unlike what we observed for the L protein, the C protein was unable to prevent PKR activation in response to poly(I:C) transfection (33), suggesting that L uses a distinct mechanism to target the PKR activation pathway.

In conclusion, our work suggests that the leader protein of TMEV acts on PKR by a novel indirect mechanism to render this kinase non-responsive to dsRNA.

Acknowledgements

We thank Stéphane Messe for technical assistance and Melissa Drappier for providing PKR phosphorylation data.

FB was the recipient of a FRIA fellowship and was further supported by a fellowship from the University of Louvain, secteur santé and by the Interuniversitary Attraction Poles programme initiated by the Belgian Science Policy Office (IAP-P7/45 BELVIR).

TC was supported by the Eranet Neuron program and is the recipient of an Aspirant fellowship of the FNRS. This work was supported by the IAP P7/45-BELVIR, the EOS joint programme of Fonds de la recherche scientifique - FNRS and Fonds wetenschapellijk onderzoek – Vlaanderen - FWO (EOS ID: 30981113), the National Lotery via the de Duve Institute and by the Belgian fund for Scientific Research (PDR T.0185.14 and CDR J.0143.18).

References

1. **Brahic M, Bureau JF, Michiels T.** 2005. The genetics of the persistent infection and demyelinating disease caused by Theiler's virus. Annu Rev Microbiol **59:**279-298.
2. **Oleszak EL, Chang JR, Friedman H, Katsetos CD, Platsoucas CD.** 2004. Theiler's virus infection: a model for multiple sclerosis. Clinical microbiology reviews **17:**174-207.
3. **Freundt EC, Drappier M, Michiels T.** 2018. Innate Immune Detection of Cardioviruses and Viral Disruption of Interferon Signaling. Frontiers in microbiology **9:**2448.
4. **van Pesch V, van Eyll O, Michiels T.** 2001. The leader protein of Theiler's virus inhibits immediate-early alpha/beta interferon production. J Virol **75:**7811-7817.
5. **Kong WP, Ghadge GD, Roos RP.** 1994. Involvement of cardiovirus leader in host cell-restricted virus expression. Proceedings of the National Academy of Sciences of the United States of America **91:**1796-1800.
6. **Bardina MV, Lidsky PV, Sheval EV, Fominykh KV, van Kuppeveld FJ, Polyakov VY, Agol VI.** 2009. Mengovirus-induced rearrangement of the nuclear pore complex: hijacking cellular phosphorylation machinery. J Virol **83:**3150-3161.
7. **Ciomperlik JJ, Basta HA, Palmenberg AC.** 2015. Three cardiovirus Leader proteins equivalently inhibit four different nucleocytoplasmic trafficking pathways. Virology **484:**194-202.
8. **Ciomperlik JJ, Basta HA, Palmenberg AC.** 2016. Cardiovirus Leader proteins bind exportins: Implications for virus replication and nucleocytoplasmic trafficking inhibition. Virology **487:**19-26.

445 9. **Delhaye S, van Pesch V, Michiels T.** 2004. The leader protein of Theiler's virus
446 interferes with nucleocytoplasmic trafficking of cellular proteins. J Virol **78:**4357-
447 4362.
448 10. **Lidsky PV, Hato S, Bardina MV, Aminev AG, Palmenberg AC, Sheval EV,**
449 **Polyakov VY, van Kuppeveld FJ, Agol VI.** 2006. Nucleocytoplasmic traffic
450 disorder induced by cardioviruses. J Virol **80:**2705-2717.
451 11. **Porter FW, Bochkov YA, Albee AJ, Wiese C, Palmenberg AC.** 2006. A
452 picornavirus protein interacts with Ran-GTPase and disrupts nucleocytoplasmic
453 transport. Proceedings of the National Academy of Sciences of the United States of
454 America **103:**12417-12422.
455 12. **Ricour C, Delhaye S, Hato SV, Olenyik TD, Michel B, van Kuppeveld FJ, Gustin**
456 **KE, Michiels T.** 2009. Inhibition of mRNA export and dimerization of interferon
457 regulatory factor 3 by Theiler's virus leader protein. J Gen Virol **90:**177-186.
458 13. **Fan J, Son KN, Arslan SY, Liang Z, Lipton HL.** 2009. Theiler's murine
459 encephalomyelitis virus leader protein is the only nonstructural protein tested that
460 induces apoptosis when transfected into mammalian cells. J Virol **83:**6546-6553.
461 14. **Romanova LI, Lidsky PV, Kolesnikova MS, Fominykh KV, Gmyl AP, Sheval EV,**
462 **Hato SV, van Kuppeveld FJ, Agol VI.** 2009. Antiapoptotic activity of the
463 cardiovirus leader protein, a viral "security" protein. J Virol **83:**7273-7284.
464 15. **Porter FW, Brown B, Palmenberg AC.** 2010. Nucleoporin phosphorylation
465 triggered by the encephalomyocarditis virus leader protein is mediated by mitogen-
466 activated protein kinases. J Virol **84:**12538-12548.
467 16. **Bacot-Davis VR, Palmenberg AC.** 2013. Encephalomyocarditis virus Leader protein
468 hinge domain is responsible for interactions with Ran GTPase. Virology **443:**177-185.

17. **Ricour C, Borghese F, Sorgeloos F, Hato SV, van Kuppeveld FJ, Michiels T.** 2009. Random mutagenesis defines a domain of Theiler's virus leader protein that is essential for antagonism of nucleocytoplasmic trafficking and cytokine gene expression. J Virol **83:**11223-11232.

18. **Borghese F, Michiels T.** 2011. The leader protein of cardioviruses inhibits stress granule assembly. J Virol **85:**9614-9622.

19. **Langereis MA, Feng Q, van Kuppeveld FJ.** 2013. MDA5 localizes to stress granules, but this localization is not required for the induction of type I interferon. J Virol **87:**6314-6325.

20. **Kedersha N, Anderson P.** 2002. Stress granules: sites of mRNA triage that regulate mRNA stability and translatability. Biochem Soc Trans **30:**963-969.

21. **Onomoto K, Jogi M, Yoo JS, Narita R, Morimoto S, Takemura A, Sambhara S, Kawaguchi A, Osari S, Nagata K, Matsumiya T, Namiki H, Yoneyama M, Fujita T.** 2012. Critical role of an antiviral stress granule containing RIG-I and PKR in viral detection and innate immunity. PLoS One **7:**e43031.

22. **Ng CS, Jogi M, Yoo JS, Onomoto K, Koike S, Iwasaki T, Yoneyama M, Kato H, Fujita T.** 2013. Encephalomyocarditis virus disrupts stress granules, the critical platform for triggering antiviral innate immune responses. J Virol **87:**9511-9522.

23. **Reineke LC, Lloyd RE.** 2013. Diversion of stress granules and P-bodies during viral infection. Virology **436:**255-267.

24. **Anderson P, Kedersha N.** 2009. Stress granules. Curr Biol **19:**R397-398.

25. **Garcia MA, Meurs EF, Esteban M.** 2007. The dsRNA protein kinase PKR: virus and cell control. Biochimie **89:**799-811.

26. **Romano PR, Garcia-Barrio MT, Zhang X, Wang Q, Taylor DR, Zhang F, Herring C, Mathews MB, Qin J, Hinnebusch AG.** 1998. Autophosphorylation in

the activation loop is required for full kinase activity in vivo of human and yeast eukaryotic initiation factor 2alpha kinases PKR and GCN2. Mol Cell Biol **18:**2282-2297.

27. **Chien CY, Xu Y, Xiao R, Aramini JM, Sahasrabudhe PV, Krug RM, Montelione GT.** 2004. Biophysical characterization of the complex between double-stranded RNA and the N-terminal domain of the NS1 protein from influenza A virus: evidence for a novel RNA-binding mode. Biochemistry **43:**1950-1962.

28. **Lu Y, Wambach M, Katze MG, Krug RM.** 1995. Binding of the influenza virus NS1 protein to double-stranded RNA inhibits the activation of the protein kinase that phosphorylates the elF-2 translation initiation factor. Virology **214:**222-228.

29. **Li C, Zhu Z, Du X, Cao W, Yang F, Zhang X, Feng H, Li D, Zhang K, Liu X, Zheng H.** 2017. Foot-and-mouth disease virus induces lysosomal degradation of host protein kinase PKR by 3C proteinase to facilitate virus replication. Virology **509:**222-231.

30. **Goodman DE, Pretto CD, Krepostman TA, Carnahan KE, Spindler KR.** 2019. Enhanced Replication of Mouse Adenovirus Type 1 following Virus-Induced Degradation of Protein Kinase R (PKR). mBio **10**.

31. **Kainulainen M, Lau S, Samuel CE, Hornung V, Weber F.** 2016. NSs Virulence Factor of Rift Valley Fever Virus Engages the F-Box Proteins FBXW11 and beta-TRCP1 To Degrade the Antiviral Protein Kinase PKR. J Virol **90:**6140-6147.

32. **Pfaller CK, Mastorakos GM, Matchett WE, Ma X, Samuel CE, Cattaneo R.** 2015. Measles Virus Defective Interfering RNAs Are Generated Frequently and Early in the Absence of C Protein and Can Be Destabilized by Adenosine Deaminase Acting on RNA-1-Like Hypermutations. J Virol **89:**7735-7747.

518 33. **Takeuchi K, Komatsu T, Kitagawa Y, Sada K, Gotoh B.** 2008. Sendai virus C
519 protein plays a role in restricting PKR activation by limiting the generation of
520 intracellular double-stranded RNA. J Virol **82:**10102-10110.
521 34. **Katze MG, DeCorato D, Safer B, Galabru J, Hovanessian AG.** 1987. Adenovirus
522 VAI RNA complexes with the 68 000 Mr protein kinase to regulate its
523 autophosphorylation and activity. EMBO J **6:**689-697.
524 35. **Langland JO, Pettiford S, Jiang B, Jacobs BL.** 1994. Products of the porcine group
525 C rotavirus NSP3 gene bind specifically to double-stranded RNA and inhibit
526 activation of the interferon-induced protein kinase PKR. J Virol **68:**3821-3829.
527 36. **Gale MJ, Jr., Korth MJ, Tang NM, Tan SL, Hopkins DA, Dever TE, Polyak SJ,**
528 **Gretch DR, Katze MG.** 1997. Evidence that hepatitis C virus resistance to interferon
529 is mediated through repression of the PKR protein kinase by the nonstructural 5A
530 protein. Virology **230:**217-227.
531 37. **He B, Gross M, Roizman B.** 1997. The gamma(1)34.5 protein of herpes simplex
532 virus 1 complexes with protein phosphatase 1alpha to dephosphorylate the alpha
533 subunit of the eukaryotic translation initiation factor 2 and preclude the shutoff of
534 protein synthesis by double-stranded RNA-activated protein kinase. Proceedings of
535 the National Academy of Sciences of the United States of America **94:**843-848.
536 38. **Visser LJ, Langereis MA, Rabouw HH, Wahedi M, Muntjewerff EM, de Groot**
537 **RJ, van Kuppeveld FJM.** 2019. Essential Role of Enterovirus 2A Protease in
538 Counteracting Stress Granule Formation and the Induction of Type I Interferon. J
539 Virol **93**.
540 39. **Dong B, Niwa M, Walter P, Silverman RH.** 2001. Basis for regulated RNA
541 cleavage by functional analysis of RNase L and Ire1p. RNA **7:**361-373.

40. **Jnaoui K, Michiels T.** 1998. Adaptation of Theiler's virus to L929 cells: mutations in the putative receptor binding site on the capsid map to neutralization sites and modulate viral persistence. Virology **244:**397-404.

41. **Duke GM, Osorio JE, Palmenberg AC.** 1990. Attenuation of Mengo virus through genetic engineering of the 5' noncoding poly(C) tract. Nature **343:**474-476.

42. **Taniuchi S, Miyake M, Tsugawa K, Oyadomari M, Oyadomari S.** 2016. Integrated stress response of vertebrates is regulated by four eIF2alpha kinases. Scientific reports **6:**32886.

43. **Reineke LC, Kedersha N, Langereis MA, van Kuppeveld FJ, Lloyd RE.** 2015. Stress granules regulate double-stranded RNA-dependent protein kinase activation through a complex containing G3BP1 and Caprin1. mBio **6:**e02486.

44. **Reineke LC, Lloyd RE.** 2015. The stress granule protein G3BP1 recruits protein kinase R to promote multiple innate immune antiviral responses. J Virol **89:**2575-2589.

45. **Chang HW, Jacobs BL.** 1993. Identification of a conserved motif that is necessary for binding of the vaccinia virus E3L gene products to double-stranded RNA. Virology **194:**537-547.

46. **Sorgeloos F, Jha BK, Silverman RH, Michiels T.** 2013. Evasion of antiviral innate immunity by Theiler's virus L* protein through direct inhibition of RNase L. PLoS pathogens **9:**e1003474.

47. **Okumura A, Pitha PM, Harty RN.** 2008. ISG15 inhibits Ebola VP40 VLP budding in an L-domain-dependent manner by blocking Nedd4 ligase activity. Proceedings of the National Academy of Sciences of the United States of America **105:**3974-3979.

48. **de la Cruz-Herrera CF, Campagna M, Garcia MA, Marcos-Villar L, Lang V, Baz-Martinez M, Gutierrez S, Vidal A, Rodriguez MS, Esteban M, Rivas C.** 2014.

Activation of the double-stranded RNA-dependent protein kinase PKR by small ubiquitin-like modifier (SUMO). J Biol Chem **289:**26357-26367.

49. **Maarifi G, El Asmi F, Maroui MA, Dianoux L, Chelbi-Alix MK.** 2018. Differential effects of SUMO1 and SUMO3 on PKR activation and stability. Scientific reports **8:**1277.

50. **Okonski KM, Samuel CE.** 2013. Stress granule formation induced by measles virus is protein kinase PKR dependent and impaired by RNA adenosine deaminase ADAR1. J Virol **87:**756-766.

51. **Mannion NM, Greenwood SM, Young R, Cox S, Brindle J, Read D, Nellaker C, Vesely C, Ponting CP, McLaughlin PJ, Jantsch MF, Dorin J, Adams IR, Scadden AD, Ohman M, Keegan LP, O'Connell MA.** 2014. The RNA-editing enzyme ADAR1 controls innate immune responses to RNA. Cell reports **9:**1482-1494.

52. **Pfaller CK, Radeke MJ, Cattaneo R, Samuel CE.** 2014. Measles virus C protein impairs production of defective copyback double-stranded viral RNA and activation of protein kinase R. J Virol **88:**456-468.

Figure legends

Figure 1. TMEV-induced stress granule assembly correlates with eIF2α phosphorylation and PKR activation.

A. Confocal microscopy images showing the co-immunostaining of eIF3 (green) and of the viral capsid protein VP1 (red) in HeLa cells infected for 10h with the wild-type virus (L^{WT}) or L-mutant viruses (L^{Zn} and L^{M60V}). Note that some VP1-negative cells also display SG in the wells infected with the L-mutant viruses. This is probably due to the fact that VP1 has not

reached a detectable level at the time the cells were fixed. **B**. Western blot analysis of eIF2α and PKR phosphorylation in HeLa cells infected as in A. 3D is the viral polymerase; β-actin detection was used as an additional loading control.

Figure 2. Pharmacological inhibition of PKR prevents TMEV-induced eIF2α phosphorylation and stress granule assembly.

HeLa cells were treated with either DMSO or C16 and infected for 10 hours with the wild-type virus (L^{WT}) or L-mutant viruses (L^{Zn} and L^{M60V}). As a control, DMSO and C16-treated cells were treated with sodium arsenite (Ars) to induce PKR-independent phosphorylation of eIF2α. **A.** Western blot analysis of eIF2α and PKR phosphorylation. **B.** Confocal microscopy images showing the co-immunostaining of eIF3 (green) and the viral capsid (red).

Figure 3. PKR is responsible for TMEV-induced eIF2α phosphorylation and stress granule assembly.

A. Western blot analysis of PKR expression in HeLa cells transduced with an empty pLKO-1 lentiviral vector (control), or with lentiviral vectors (FB52, 53 and 54) expressing shRNA 1, 2 or 3, directed against PKR. Transduced cells were selected for one week with puromycin before being assessed for PKR expression. **B.** Control HeLa cells and HeLa cells transduced with FB54 (shRNA3) were infected for 10 hours with wild-type (L^{WT}) or L-mutant (L^{Zn} and L^{M60V}) viruses. Mock-infected and L^{M60V} -infected cell samples were treated for 30 min with sodium arsenite prior to cell lysis. Lysates were harvested at 10hpi and PKR expression and eIF2α phosphorylation were analyzed by Western blot. **C.** Confocal microscopy images showing the co-immunostaining of eIF3 (green) and the viral capsid (red) in control and PKR-knocked down HeLa cells infected or treated as in B.

Figure 4: L acts at two levels in the stress granule formation pathway.

A-D. L^{WT} prevents $NaAsO_2$-mediated SG assembly: HeLa cells were left uninfected (NI) of were infected for 10h with KJ6 (L^{WT}). Where indicated, cells were treated for 30 min with $NaAsO_2$ before being fixed and processed for eIF3 and VP1 immunostaining (A, D) or before protein harvest and Western blot analysis of eIF2α phosphorylation (B-C).

A. Representative confocal microscopy images showing the absence of stress granules in L^{WT}-infected $NaAsO_2$-treated cells (upper right panel). **B**. representative Western blot monitoring of eIF2α (Ser51) phosphorylation and total eIF2α in uninfected and infected cells treated with increasing concentrations of $NaAsO_2$. **C**. Quantification (mean and SD values) of the data shown in B (n=3). **D**. Percentage (mean and SD values) of SG-positive cells, among infected cells, as counted from microscopy images taken from uninfected or infected $NaAsO_2$-treated cells (n=3).

E-F. TMEV and mengovirus L^{WT} proteins can inhibit PKR activation: HeLa cells were infected with L^{WT} or indicated L mutant viruses (12h, 2 PFU per cell for TMEV; 6h, 5 PFU per cell for mengovirus). phospho-PKR (Thr446) and total PKR were quantified by Western blot (mean and SD values; n=5 for TMEV, n=4 for mengovirus).

* ($p<0.05$), **($p<0.01$), ***($p<0.001$), ANOVA comparisons.

Figure 5: PKR is a strong antagonist of TMEV replication.

Control- or $PKR^{Knock\text{-}Down}$ - HeLa cells were infected with wild-type virus (L^{WT}) or L-mutant (L^{Zn} and L^{M60V}) viruses and supernatants were harvested at 16 hours post-infection. Viral titers were measured by plaque assay. Histograms show the mean and SD values of three independent infection experiments.

Figure 6. L prevents the interaction between viral dsRNA and PKR.

A. HeLa cells were infected with 5PFU per cell of TM994, TM1016 and TM1017, recombinant TMEV expressing 3xFLAG-L^{WT}, 3xFLAG-L^{Zn} and 3xFLAG-L^{M60V} respectively. At 10 hpi, cells were lysed and 3xFLAG-L proteins were immunoprecipitated using an anti-FLAG antibody. The presence of L (FLAG detection), PKR, phospho-PKR (Thr446) and G3BP1 was assessed by Western blot in cell lysates (ly), in post-IP lysate fractions (ly_p) and in immunoprecipitates (IP). **B.** Confocal microscopy images showing the co-immunostaining of dsRNA and PKR in HeLa cells infected for 10 hours with wild-type (L^{WT}) or L-mutant (L^{Zn} and L^{M60V}) viruses and of PKR. Note the marked redistribution of PKR to punctate structures in cells infected with the L-mutant viruses.

C. Confocal microscopy images showing the co-immunostaining of PKR, eIF3 and G3BP (left panels) and of PKR, eIF3 and dsRNA (right panels) in HeLa cells infected as in B, with the L^{M60V} mutant virus. **D**. cartoon summarizing the observations. **E.** HeLa cells were infected for 10 hours with the wild-type or L-mutant viruses, or transfected with poly(I:C) for 4 hours, before lysis and dsRNA immunoprecipitation. The presence of PKR, phospho-PKR, and L was monitored by Western blot in equivalent amounts of whole-cell lysates and IP products. Graphs show the mean and SD values of PKR amounts detected in lysates and dsRNA immunoprecipitated fractions from 3 experiments. * ($p<0.05$) for ANOVA pairwise comparisons between lysates and IP fractions.

Figure 7: L affects the responsiveness of PKR to dsRNA.

A-B. HeLa cells were infected with the wild-type (L^{WT}) and L^{Zn}-mutant viruses. At 6 hpi, cells were transfected with 500 ng of poly(I:C) or control-treated with the transfection reagent only. At 10 hpi whole-cell lysates were harvested and analyzed by Western blot to monitor PKR phosphorylation on threonine 446 and 451. **B**. Quantification of the phospho-

Thr446/total PKR ratio from 3 experiments (mean and SD values). * ($p<0.05$), **($p<0.01$), ***($p<0.001$) for ANOVA comparisons.

C-D. HeLa cells were infected for 10 hours with the wild-type virus (L^{WT}) or with a mutant virus that expresses GFP instead of L (ΔL-GFP), or were co-infected with both viruses. PKR phosphorylation was assessed by Western blot (C), and its distribution was monitored by classical immunofluorescent microscopy (D). White arrows indicate infected cells presenting a typical punctate redistribution of PKR.

Table 1. Viruses used in this study

TMEV derivatives

VIRUS[1]	PARENTAL	CHARACTERISTICS
KJ6	DA1	L^{WT} ; capsid adapted to L929 cells
TM659	KJ6	L^{Zn} ; capsid adapted to L929 cells
FB09	KJ6	L^{M60V} ; capsid adapted to L929 cells
KJ7	KJ6	ΔL-GFP ; capsid adapted to L929 cells
TM994	KJ6	3xFLAG-L^{WT} ; capsid adapted to L929 cells
TM1016	KJ6	3xFLAG-L^{Zn} ; capsid adapted to L929 cells
TM1017	KJ6	3xFLAG-L^{M60V} ; capsid adapted to L929 cells

mengovirus derivatives

VIRUS[1]	PARENTAL	CHARACTERISTICS
FS269	MC24	FLAG-L^{WT}; 5' polyC tract reduced (24C)
TM1097	FS269	FLAG-L^{Zn} (C19A-C22A) double mutation in L

Lentiviral vectors

VIRUS	PARENTAL	CHARACTERISTICS
FB52	pLKO.1	shRNA 1 PKR : TRCN0000001379; puromycin resistance
FB53	pLKO.1	shRNA 2 PKR : TRCN0000001381; puromycin resistance
FB54	pLKO.1	shRNA 3 PKR : TRCN0000196400; puromycin resistance

[1]. Plasmid carrying the corresponding full-length cDNA are designed with an additional « p » (i.e. plasmid pKJ6 for virus KJ6)

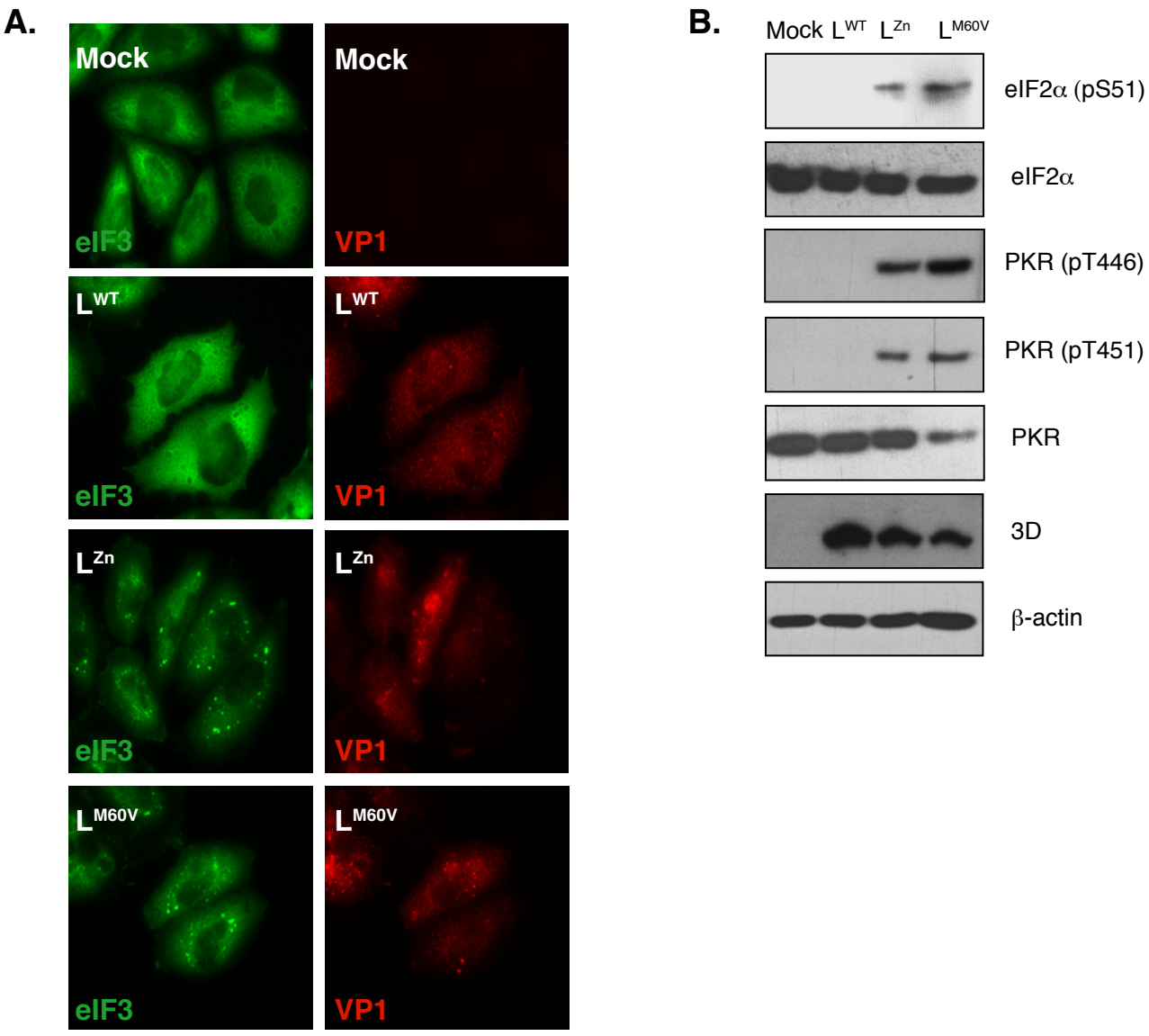

Figure 1: TMEV-induced stress granule assembly correlates with eIF2α phosphorylation and PKR activation.

A. Confocal microscopy images showing the co-immunostaining of eIF3 (green) and of the viral capsid protein VP1 (red) in HeLa cells infected for 10h with the wild-type virus (L^{WT}) or L-mutant viruses (L^{Zn} and L^{M60V}).
B. Western blot analysis of eIF2α and PKR phosphorylation in HeLa cells infected as in A. 3D is the viral polymerase; β-actin detection was used as an additional loading control.
.

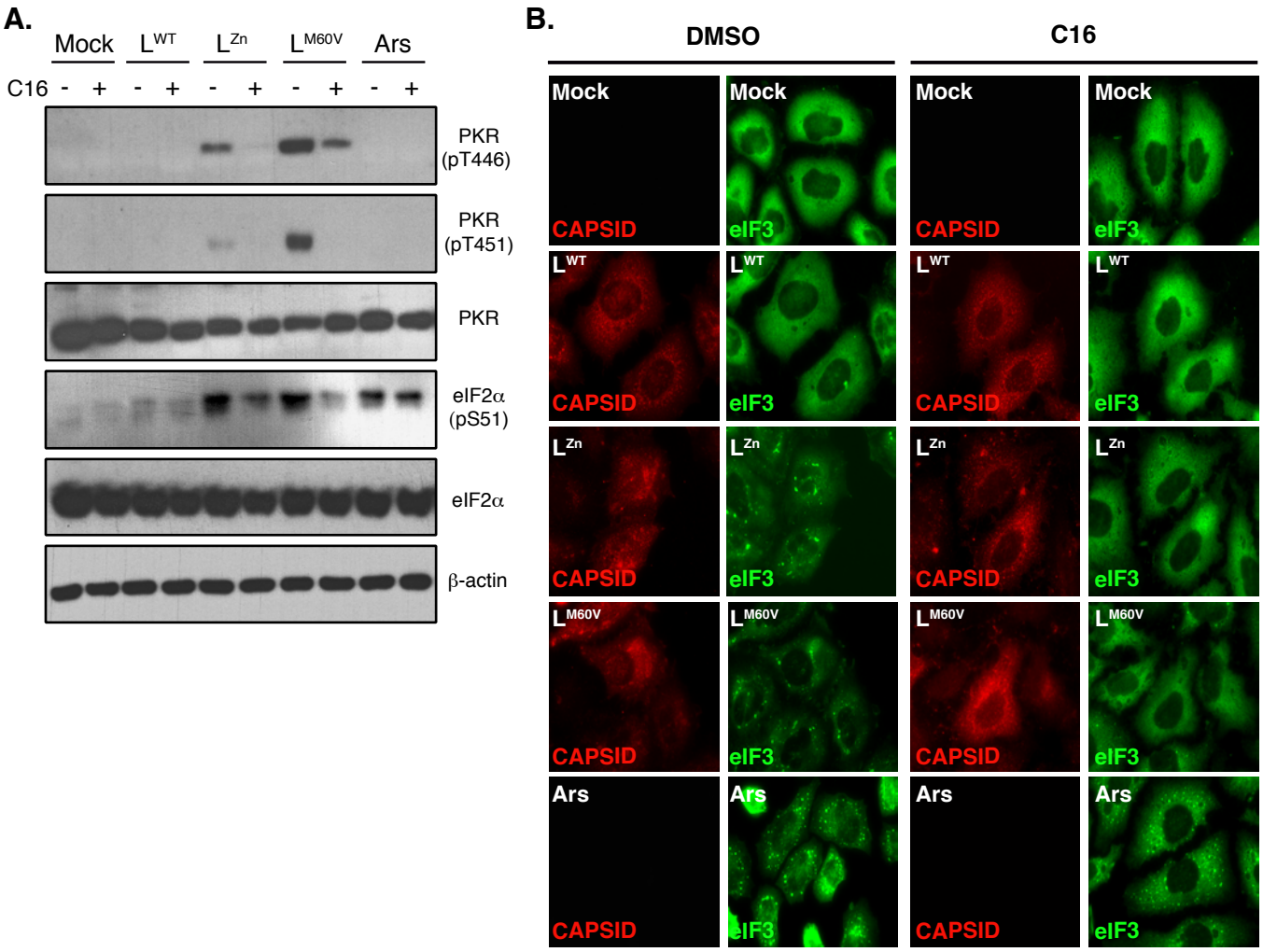

Figure 2: Pharmacological inhibition of PKR prevents TMEV-induced eIF2α phosphorylation and stress granule assembly.

HeLa cells were treated with either DMSO or C16 and infected for 10 hours with the wild-type virus (L^{WT}) or L-mutant viruses (L^{Zn} and L^{M60V}). As a control, DMSO and C16-treated cells were treated with sodium arsenite (Ars) to induce PKR-independent phosphorylation of eIF2α.
A. Western blot analysis of eIF2α and PKR phosphorylation.
B. Confocal microscopy images showing the co-immunostaining of eIF3 (green) and the viral capsid (red).

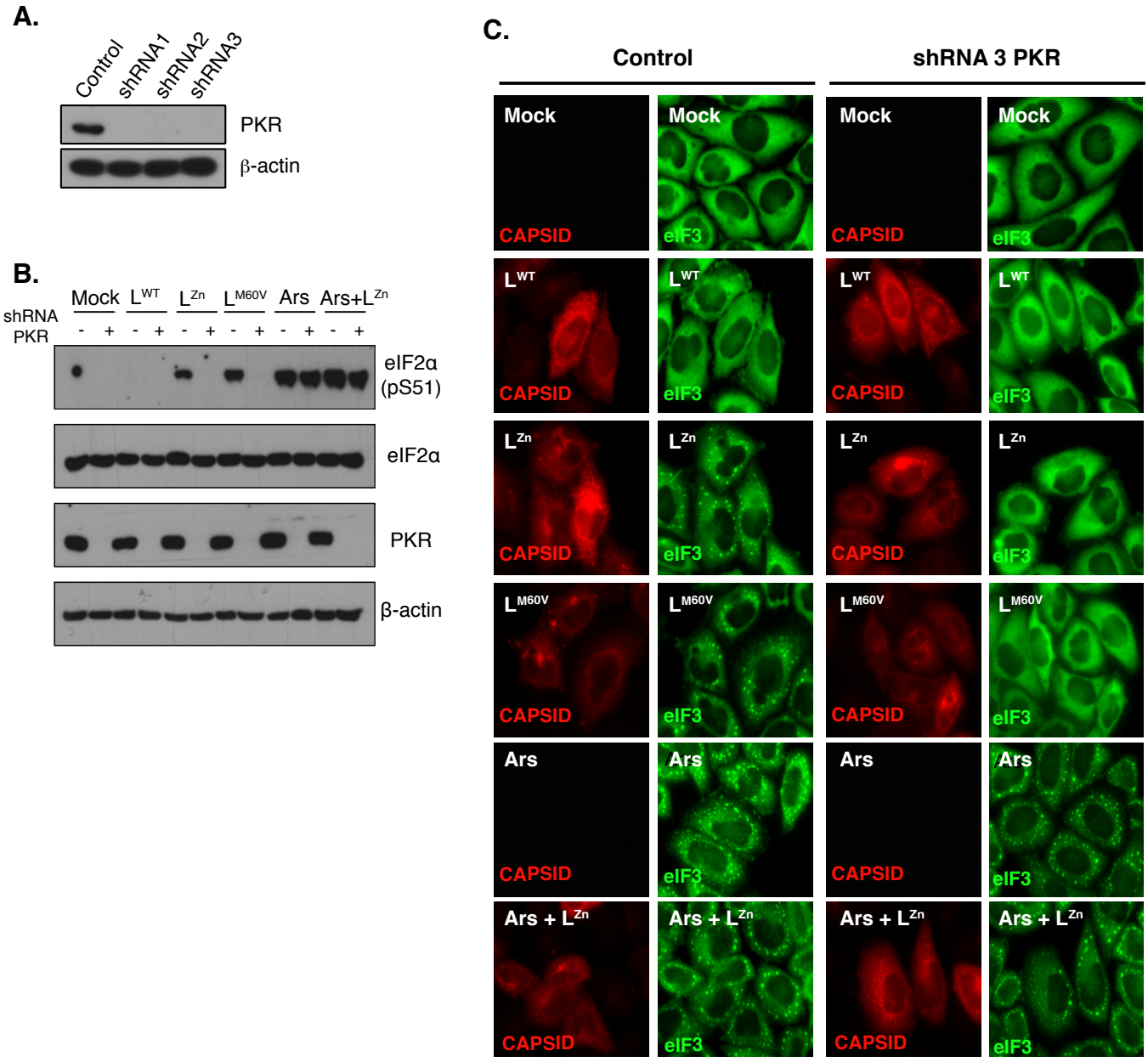

Figure 3: PKR is responsible for TMEV-induced eIF2α phosphorylation and stress granule assembly.

A. Western blot analysis of PKR expression in HeLa cells transduced with an empty pLKO-1 lentiviral vector (control), or with lentiviral vectors (FB52, 53 and 54) expressing shRNA 1, 2 or 3, directed against PKR. Transduced cells were selected for one week with puromycin before being assessed for PKR expression.
B. Control HeLa cells and HeLa cells transduced with FB54 (shRNA3) were infected for 10 hours with wild-type (L^{WT}) or L-mutant (L^{Zn} and L^{M60V}) viruses. Mock-infected and L^{M60V} -infected cell samples were treated for 30 min with sodium arsenite prior to cell lysis. Lysates were harvested at 10hpi and PKR expression and eIF2α phosphorylation were analyzed by Western blot.
C. Confocal microscopy images showing the co-immunostaining of eIF3 (green) and the viral capsid (red) in control and PKR-knocked down HeLa cells infected or treated as in B.

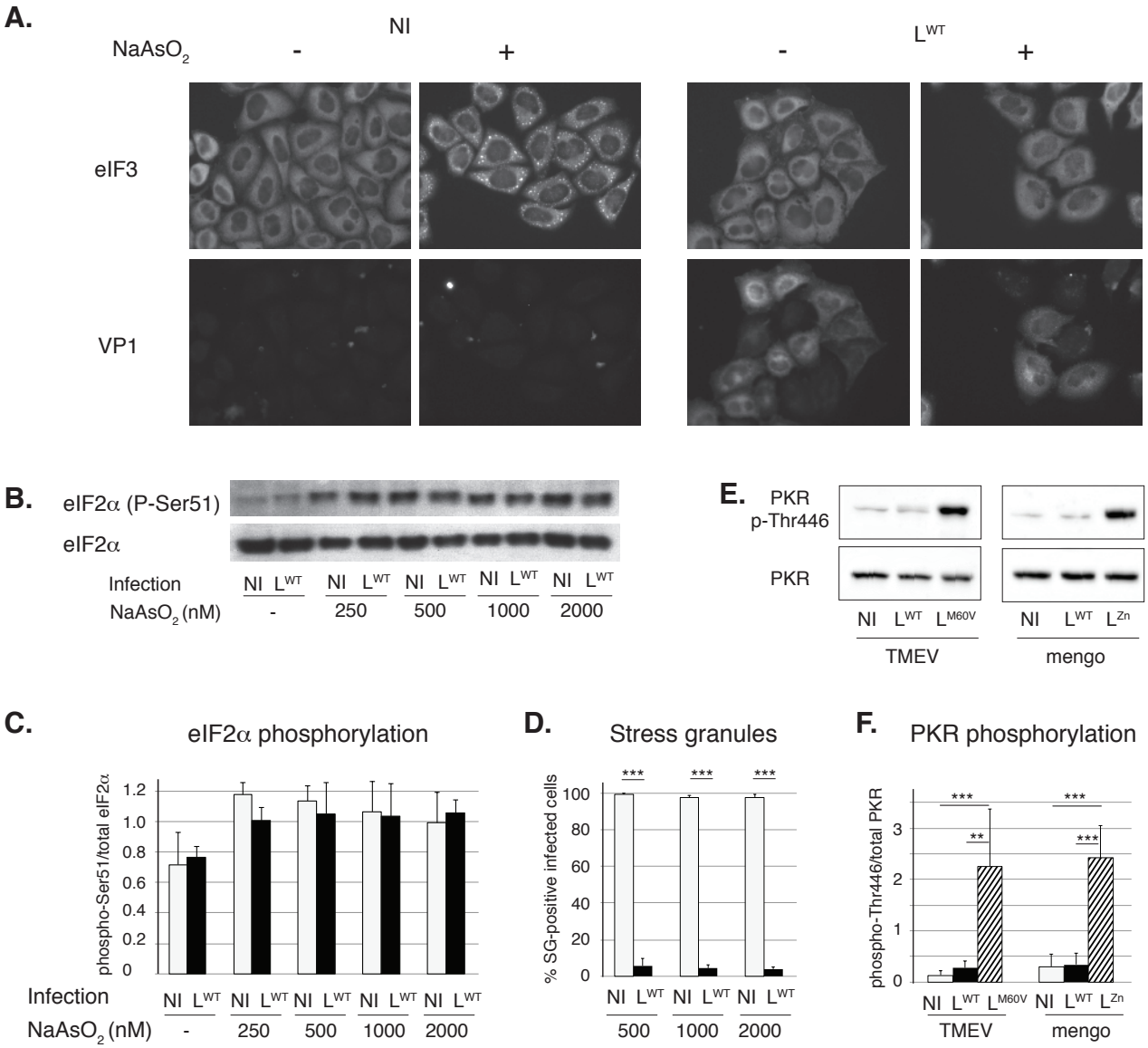

Figure 4: L acts at two levels in the stress granule formation pathway.

A-D. L^{WT} prevents $NaAsO_2$-mediated SG assembly: HeLa cells were left uninfected (NI) of were infected for 10h with KJ6 (L^{WT}). Where indicated, cells were treated for 30 min with $NaAsO_2$ before being fixed and processed for eIF3 and VP1 immunostaining (A, D), or before protein harvest and western blot analysis of eIF2 α phosphorylation (B-C).

A. Representative confocal microscopy images showing the absence of stress granules in L^{WT}-infected $NaAsO_2$-treated cells (upper right panel).

B. representative (n=3) Western blot monitoring of eIF2α (Ser51) phosphorylation and total eIF2α in uninfected and infected cells treated with increasing concentrations of $NaAsO_2$.

C. Quantification (mean and SD) of eIF2α phosphorylation from experiments as shown in B (n=3).

D. Percentage (mean and SD) of SG-positive cells among infected cells, as counted from microscopy images taken from uninfected or infected $NaAsO_2$-treated cells (n=3).

E-F. TMEV and mengovirus L^{WT} proteins can inhibit PKR activation: HeLa cells were infected with L^{WT} or indicated L mutant viruses (12h, 2 PFU per cell for TMEV; 6h, 5 PFU per cell for mengovirus). phospho-PKR (Thr446) and total PKR were quantified by western blot (mean and SD; n=5 for TMEV, n=4 for mengovirus). * ($p<0.05$), **($p<0.01$), ***($p<0.001$) ANOVA comparisons.

.

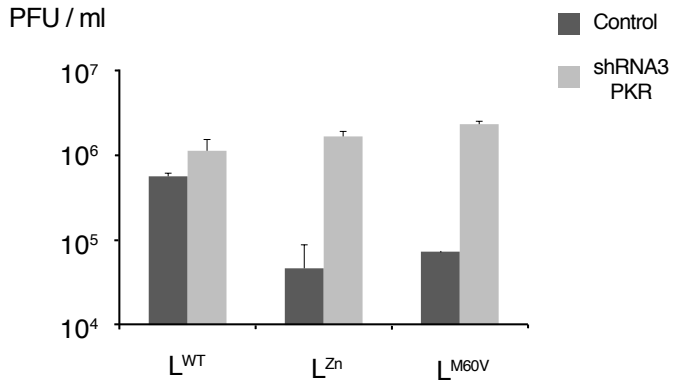

Figure 5: PKR is a strong antagonist of TMEV replication.

Control- or $PKR^{Knock\text{-}Down}$ - HeLa cells were infected with wild-type virus (L^{WT}) or L-mutant (L^{Zn} and L^{M60V}) viruses and supernatants were harvested at 16 hours post-infection. Viral titers were measured by plaque assay. Histograms show the mean and SD values of three independent infection experiments.

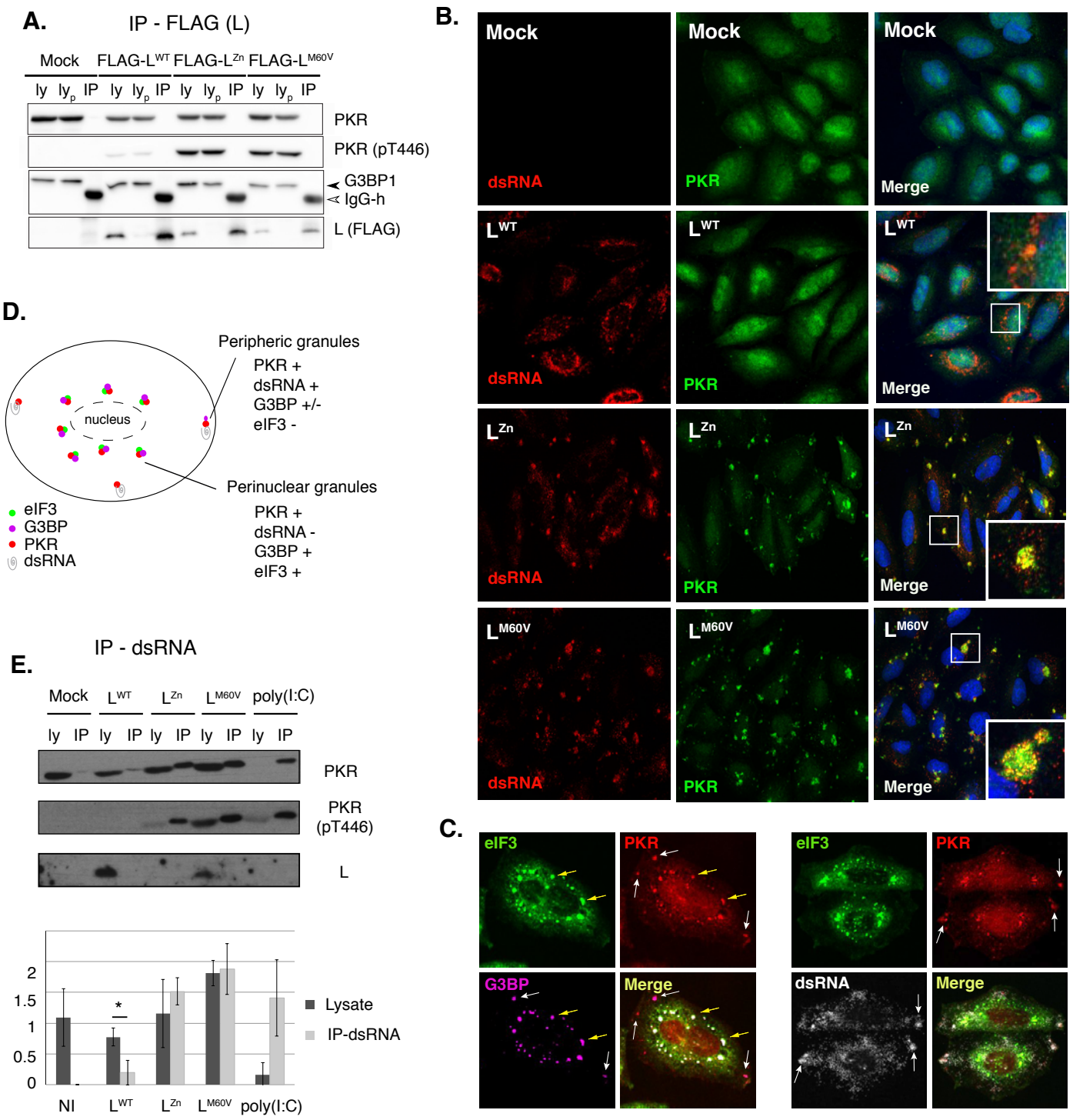

Figure 6: L prevents the interaction between viral dsRNA and PKR.

A. HeLa cells were infected with 5 PFU per cell of TM994, TM1016 and TM1017, recombinant TMEV expressing 3xFLAG-L^{WT}, 3xFLAG-L^{LZ}n and 3xFLAG-^{LM60}V respectively. At 10 hpi, cells were lysed and 3xFLAG-L proteins were immunoprecipitated using an anti-FLAG antibody. The presence of L (FLAG detection), PKR, phospho-PKR (Thr446) and G3BP1 was assessed by Western blot in cell lysates (ly), in post-IP lysate fractions (l_yp) and in immunoprecipitates (IP)

B. Co-immunostaining of dsRNA (red) and PKR (green) in HeLa cells infected for 10 hours with wild-type (L^{WT}) or L-mutant (L^{Zn} and L^{M60V}) viruses and of PKR. Note the marked redistribution of PKR to punctate structures in cells infected with the L-mutant viruses.

C. Confocal microscopy images showing the co-immunostaining of PKR, eIF3 and G3BP (left panels) and of PKR, eIF3 and dsRNA (right panels) in HeLa cells infected as in B, with the L^{M60V} mutant virus.

D. cartoon summarizing the observations.

E. HeLa cells were infected for 10 hours with the wild-type or L-mutant viruses, or transfected with poly(I:C) for 4 hours, before lysis and dsRNA immunoprecipitation. The presence of PKR, phospho-PKR, and L was monitored by Western blot in equivalent amounts of whole-cell lysates and IP products. Graphs show the mean and SD of PKR detection in lysates and dsRNA immunoprecipitated fractions from 3 experiments.

* ($p<0.05$) for ANOVA pairwise comparisons between lysates and IP fractions.

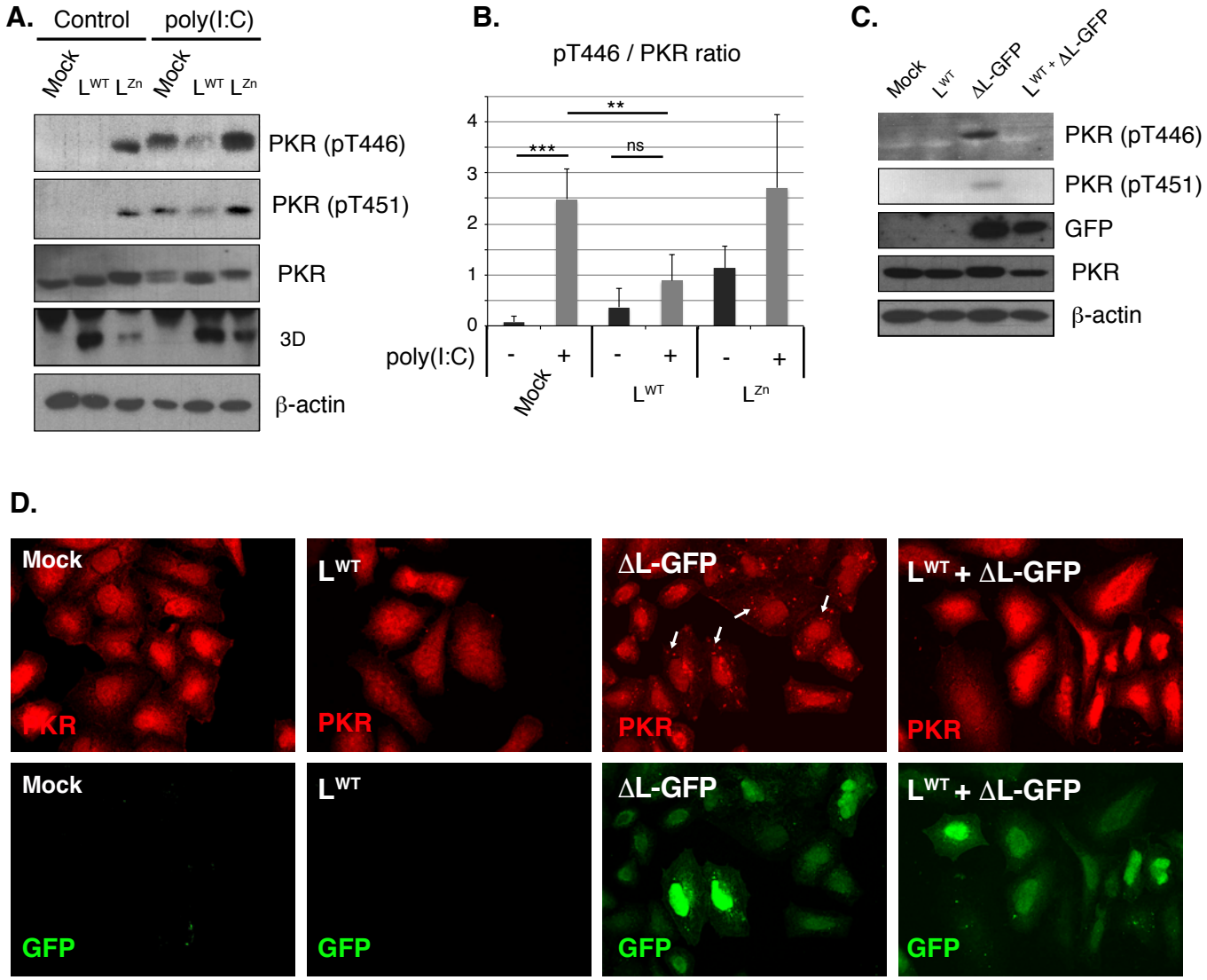

Figure 7: L affects the responsiveness of PKR to dsRNA.

A-B. HeLa cells were infected with the wild-type (L^{WT}) and L^{Zn}-mutant viruses. At 6 hpi, cells were transfected with 500 ng of poly(I:C) or control-treated with the transfection reagent only. At 10 hpi whole-cell lysates were harvested and analyzed by Western blot to monitor PKR phosphorylation on threonine 446 and 451.
B. Quantification of the phospho-Thr446/total PKR ratio from 3 experiments (mean and SD). * ($p<0.05$), **($p<0.01$), ***($p<0.001$) for ANOVA comparisons.
C-D. HeLa cells were infected for 10 hours with the wild-type virus (L^{WT}) or with a mutant virus that expresses GFP instead of L (ΔL-GFP), or were co-infected with both viruses. PKR phosphorylation was assessed by Western blot (C), and its distribution was monitored by classical immunofluorescent microscopy (D). White arrows indicate infected cells presenting a typical punctate redistribution of PKR.